Article | Received 21 January 2026; Revised 18 March 2026; Accepted 10 April 2026; Published 8 May 2026
https://doi.org/10.55092/aimat20260005

Towards signal-based estimation of contact tip–to–workpiece distance (CTWD) in wire arc directed energy deposition via 1D convolutional deep learning

Giulio Mattera[1,*], Elena Manoli[1], Luigi Nele[1] and Jinyang Xu[2]

[1] Department of Chemical, Materials and Production Engineering, University of Naples "Federico II", Naples, Italy
[2] Faculty of Intelligence Technology, Shanghai Institute of Technology, Shanghai, China

* Correspondence author; E-mail: giulio.mattera@unina.it.

Highlights:

- Indirect measurement of CTWD during the WA-DED process with high-frequency welding signals.
- Discussion of the potential usage of the proposed process monitoring application.

Abstract: In open-loop Wire Arc Directed Energy Deposition (WA-DED), the contact tip–to–workpiece distance (CTWD) is commonly adjusted between layers using expected average values of layer height derived from experimental data. However, due to complex thermal effects, mismatches between expected and actual process conditions lead to uncontrolled CTWD fluctuations, which can cause process instabilities, arc extinction events, and geometric defects. Reliable online estimation of CTWD is therefore essential for process monitoring and for enabling future closed-loop control strategies. Existing CTWD monitoring approaches typically rely on vision-based or acoustic emission systems, which are costly or sensitive to industrial noise. This work proposes a data-driven method for online CTWD estimation using only welding current and voltage, signals already available in industrial WA-DED systems. By avoiding additional sensors, the approach enables low-cost, robust, and real-time CTWD estimation suitable for direct industrial deployment. Several machine learning and deep learning models are evaluated, with particular focus on Ridge Regression, Support Vector Regression and a 1-dimensional convolutional neural network. Experimental results show that the deep learning approach provides higher estimation accuracy and robustness compared to conventional machine learning methods, while remaining suitable for real-time implementation. The proposed method offers a practical solution for CTWD monitoring in WA-DED and represents a step towards intelligent process supervision and control in wire-based additive manufacturing.

Keywords: wire arc directed energy deposition; online process monitoring; deep learning; process stability; closed-loop control; additive manufacturing; artificial intelligence

1. Introduction

Wire Arc Directed Energy Deposition (WA-DED) (see Figure 1) is an additive manufacturing process for metallic components that has gained increasing attention in industrial contexts. Its attractiveness lies in the capability to fabricate large-scale parts with high deposition rates, using a wide range of alloys, while relying on mature welding hardware without fundamental changes to the underlying process physics or machine architecture [1−3]. These characteristics make WA-DED particularly suitable for structural components, repair applications [4], and low-to-medium complexity geometries where productivity and material efficiency are critical. In WA-DED, once the CAD model of the part is defined, a slicing algorithm discretises the geometry into a sequence of layers. The distance between successive slices is determined by an estimated layer height, which is commonly obtained from preliminary experiments performed under fixed and controlled process parameters. In practice, a wall is deposited under steady-state conditions, and the average measured layer height (h) is then used as a reference value for slicing the entire component [5].

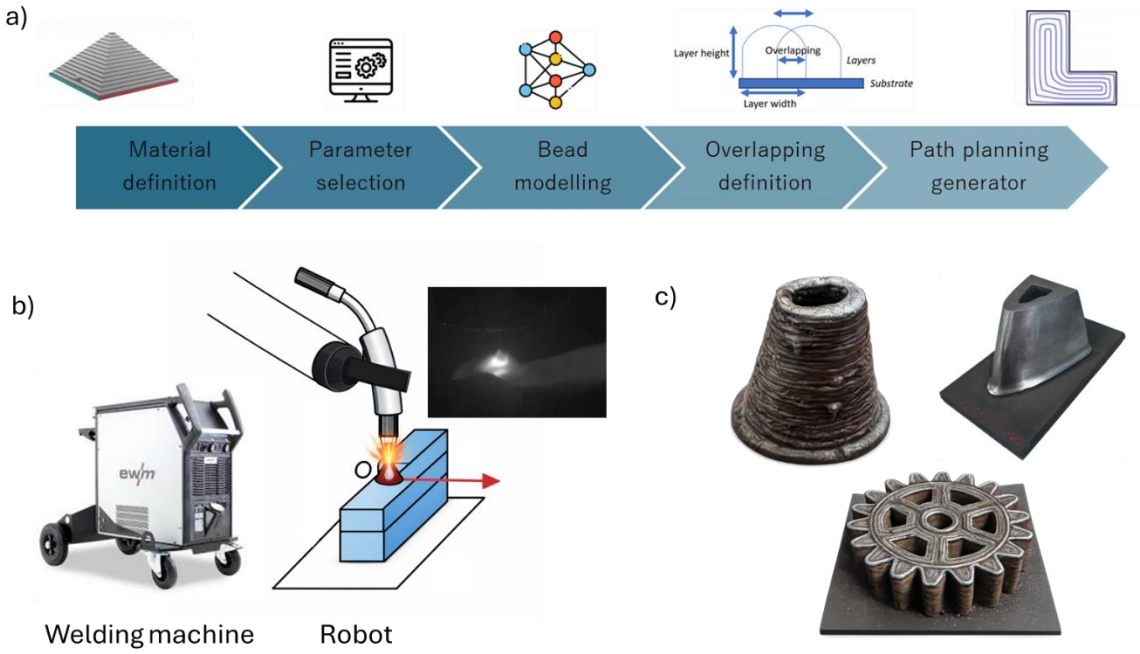

Figure 1. Schematic overview of the Wire Arc Direct Energy Deposition process: **(a)** Workflow; **(b)** Process physics and equipment; **(c)** Typical final products.

Therefore, the next layer is deposited using the estimated layer height, but the deposited layer geometry is inherently variable and evolves during the build process due to thermal accumulation [6,7], introducing changes in the contact tip–to–workpiece distance (CTWD). These variations directly affect arc length, heat input, metal transfer behaviour, and arc stability, often resulting in arc extinction events, geometric inconsistencies, and process interruptions that require manual intervention [8]. For these reasons, the online estimation and control of CTWD have been widely recognised as key enablers for improving process stability and build quality in WA–DED [9].

Some studies have investigated CTWD estimation using indirect sensing approaches, including linear regression models based on acoustic emission signals [10] or image–based measurements acquired from welding cameras [11]. While these methods have demonstrated feasibility, they often rely on costly sensing

hardware (e.g. welding camera) or are sensitive to environmental noise (e.g. microphones), limiting their robustness and industrial applicability. This context motivates the development of data-driven CTWD estimation methods based on low-cost, readily available process signals, such as welding current and voltage, with the aim of enabling reliable online monitoring and potentially moving towards an effective closed-loop control of the WA-DED process.

Artificial Intelligence (AI), particularly machine learning (ML), is increasingly employed in materials science and related engineering disciplines to tackle complex problems [12,13], including those addressed in this work, by enabling effective analysis of high-frequency process data beyond the capabilities of conventional modelling approaches. In WA–DED, welding current and voltage signals are typically acquired at sampling frequencies exceeding 5 kHz, posing challenges for simple linear regression models due to the volume, temporal complexity, and non-stationary nature of the data [14]. In this work, different data-driven methods are investigated for CTWD estimation. With respect to classical ML approaches, Ridge Linear Regression (RLR) and Support Vector Regression (SVR) are considered. In these cases, representative features are extracted online from the time-domain welding signals and used as inputs to estimate the CTWD value in millimetres based on measurements of welding current and voltage. In addition, a more advanced Deep Learning (DL) approach is proposed and comparatively analysed. Specifically, a one-Dimensional Convolutional Neural Network (1D–CNN) is employed to directly process raw welding signals. This architecture has demonstrated effectiveness in previous monitoring tasks involving similar one-dimensional signals [15], including anomaly detection and process stability assessment. By operating directly on raw data, the proposed approach eliminates the need for manual feature extraction, enabling end-to-end learning and improving robustness under varying process conditions.

Overall, the proposed framework provides a systematic assessment of both ML and deep learning strategies for CTWD estimation, demonstrating the feasibility of accurate real–time monitoring based solely on high-frequency electrical welding signals. Such a comparison allows one to evaluate whether linear, non-linear, or more complex modelling approaches are most appropriate when learning directly from raw process data. In this sense, the present work moves towards the development of a signal–driven methodology, showing how process monitoring based on electrical welding signals can support the identification of out-of-specification conditions during WA-DED.

2. Methods

2.1. Experimental setup and certification-oriented paradigm

In this study, experimental data were collected using an integrated WA-DED cell (see Figure 2) comprising an ABB IRB 2600 robotic arm equipped with an EWM Titan XQ 400 Plus welding power source. The system is instrumented with welding current and voltage sensors, acquiring data at a sampling frequency of 5 kHz. The material under investigation is Invar 36 alloy, which is gaining increasing interest in additive manufacturing, owing to its high thermal stability and the challenges associated with its machining using conventional processes [16–20]. The feedstock consists of a 1.2 mm diameter wire. A preliminary experimental campaign was conducted to identify a stable deposition window under natural short-circuit transfer mode [5]. The optimal process parameters were determined as wire feed speed equal to 6 m/min, welding speed of 7.5 mm/s, reference welding voltage of 20 V,

argon shielding gas flow rate of 12.5 L/min, and a fixed CTWD of 13 mm. Based on these parameters, the experimental campaign was conducted using this parameter set as the reference condition, as it ensures high build quality and process stability.

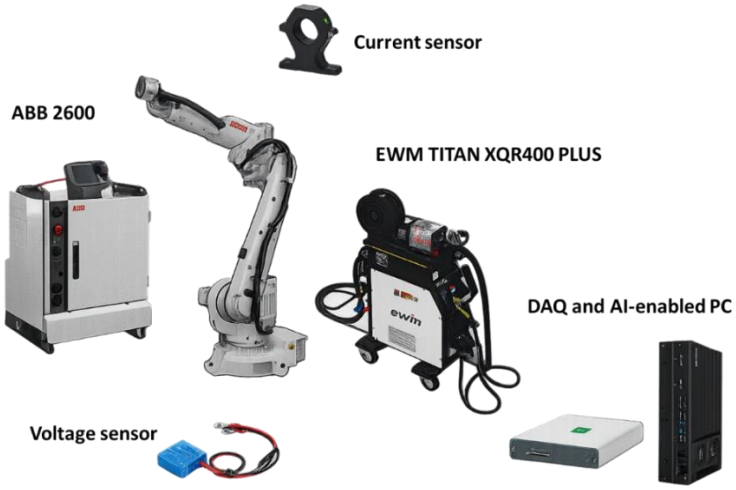

Figure 2. Experimental setup comprising an ABB IRB 2600 robotic platform and an EWM welding system, with welding current and voltage acquired through a NI USB-6361 device and streamed to an AI-enabled workstation.

The objective of this study is to define guidelines for the development of CTWD estimators under certified process conditions. Therefore, following the certification-oriented paradigm [14], once optimal parameters are selected, the main objective is that the process must be maintained within the qualified operating window, ensuring compliance with certification requirements. In this context, continuous monitoring during production becomes essential to ensure that the final component remains within the certified operating envelope. The proposed CTWD estimation method provides a means to detect unstable process conditions arising from deviations with respect to certified CTWD values, while also enabling the implementation of feedback control strategies.

Moreover, adopting a certification-oriented paradigm reduces data variability during model development, enabling the construction of reliable models even when only medium-sized datasets are available. Moreover, this approach allows different CTWD estimation models to be trained for distinct qualified parameter sets, facilitating seamless switching between configurations without affecting the general applicability of the proposed methodology. Ultimately, the proposed method supports quality monitoring during deposition and enables the implementation of dedicated feedback control strategies to maintain the process within certification limits.

2.2. Data collection

The data collection procedure was designed following a systematic and controlled approach, using the previously identified optimal and certified process parameter set. These parameters were kept constant throughout the experiments in order to isolate the effect of variations in the CTWD on the welding signal time series. From a dynamic system identification perspective, step-response analysis is a widely adopted methodology for characterising system dynamics. Accordingly, the experimental campaign was structured by introducing discrete and controlled CTWD variations within single deposited layers,

allowing both transient and steady-state process responses to be observed. In total, 4 deposition layers were produced, each characterised by a sequence of CTWD steps applied along the deposition path.

In the first layer, CTWD values of 9.5, 11.5, 12.5, 13.5, and 15.5 mm were imposed, with each step extending over a deposition length of 50 mm. The second layer consisted of CTWD steps of 8.5, 12.5, 16.5, 17.5, and 18.5 mm, again applied over 50 mm intervals. In the third layer, CTWD values of 8.5, 10.5, 13.5, 15.5, and 18.5 mm were employed, while the fourth layer introduced two larger step variations at 11 and 19 mm to investigate more pronounced dynamic transitions. Overall, 17 CTWD steps were analysed across the four layers. The summary of the data collection procedure is reported in Table 1.

Table 1. Summary of CTWD step-response experimental design

Layer	CTWD step values (mm)	Number of steps	Step length (mm)
Layer 1	9.5, 11.5, 12.5, 13.5, 15.5	5	50
Layer 2	8.5, 12.5, 16.5, 17.5, 18.5	5	50
Layer 3	8.5, 10.5, 13.5, 15.5, 18.5	5	50
Layer 4	11, 19	2	50
Total	-	17	-

Welding current and voltage signals were acquired continuously during deposition. To remove non-representative process phases, the initial and final portions of each signal segment were discarded in order to eliminate the effects of arc ignition and arc extinction. The remaining time series were then segmented into fixed-length temporal windows of 200 ms, each containing 1000 samples. As shown in Figure 3, variations in the CTWD directly affect the heat input, resulting in measurable changes in the amplitude and temporal characteristics of the welding signal time series.

A quantitative analysis further confirms this relationship. The Spearman rank correlation between CTWD and the corresponding heat input computed from current and voltage signals is $\rho = -0.83$ ($p < 10^{-180}$), indicating a strong monotonic dependency between the CTWD and the heat input delivered during the process.

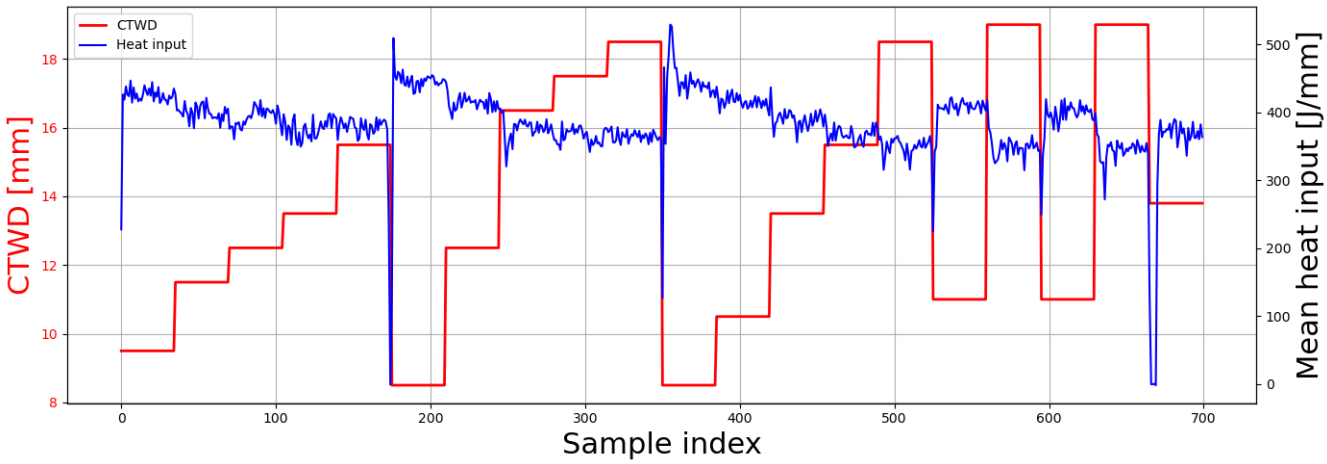

Figure 3. Reference CTWD and corresponding heat input computed from welding current and voltage signals, showing that variations in CTWD are associated with changes in welding waveforms and therefore of the heat input magnitude.

This behaviour highlights not only the strong correlation between electrical welding signals and CTWD, but also the critical role of CTWD monitoring in maintaining a stable thermal regime during the deposition process. When CTWD deviates from certified reference values, unintended variations in heat input arise, potentially leading to process instabilities and geometric inconsistencies. In a certification-oriented production framework, such uncontrolled thermal fluctuations may result in non-compliant components. Consequently, reliable online CTWD estimation is essential to ensure consistent heat input and to preserve process conditions within certified operating windows.

The resulting dataset was constructed by concatenating the welding current and voltage signals into a three-dimensional input tensor of shape (700, 2, 1000), where 700 denotes the total number of samples, 2 represents the input channels (current and voltage), and 1000 corresponds to the number of time steps per sample. Since the imposed CTWD values were known a priori for each step, the corresponding output variable was explicitly defined for every sample. Consequently, the dataset is fully labelled and suitable for supervised learning, enabling the direct development and validation of CTWD estimation models.

2.3. Machine learning methods

In this work, the estimation of the CTWD is formulated as a supervised learning problem aimed at mapping high-frequency electrical welding signals to the corresponding CTWD value. More specifically, the input consists of the welding current and voltage time series, while the output is the CTWD associated with each observation window. To investigate how this sensor-to-estimation mapping can be modelled, three different regression strategies are considered, spanning increasing levels of modelling complexity and representational capability. These include classical machine learning approaches based on manually extracted features, as well as a deep learning approach capable of learning directly from raw signal time series. This comparison is intended to assess not only predictive accuracy, but also the extent to which increasingly expressive models can capture the underlying relationship between welding dynamics and CTWD.

Regarding the ML approach, it is formulated as a two-stage process consisting of feature extraction from high-frequency welding signal time series, followed by regression-based estimation of the CTWD. Let

$$\mathbf{x}_i(t) = [I_i(t), V_i(t)] \tag{1}$$

denote the welding current and welding voltage signals associated with the i-th observation, in this case study every 200 ms of deposition. In a classical ML framework, these signals are transformed into a fixed-dimensional feature vector through a deterministic mapping

$$\boldsymbol{\phi}_i = \mathcal{F}(\mathbf{x}_i), \tag{2}$$

where $\boldsymbol{\phi}_i \in \mathbb{R}^p$. In this study, $\mathcal{F}(\cdot)$ it is a function that extracts time-domain statistical features, such as mean and variance, as well as frequency-domain descriptors derived from the magnitude spectrum of the fast Fourier transform (FFT), again considering mean and variance. These features capture both temporal amplitude variations and spectral characteristics of the welding signals and have been extensively used in previous studies addressing process monitoring in WA-DED [21–23]. The extracted features ($\boldsymbol{\phi}_i^8$) are listed in Table 2.

Table 2. Feature set adopted for the ML-based CTWD estimation models.

Signal	Time-domain features	Frequency-domain features
Welding current	Mean, variance	Mean and variance of FFT magnitude
Welding voltage	Mean, variance	Mean and variance of FFT magnitude

Given the extracted features, the regression task consists of estimating the CTWD value y_i, obtained as described in previous section. The scikit-learn python library has been used for development and deploy on the industrial PC connected to the NI DAQ system described in the previous section. For linear modelling, RLR is employed, which assumes a linear relationship

$$\hat{y}_i = \boldsymbol{\phi}_i^{\top}\boldsymbol{\beta}, \tag{3}$$

where the regression coefficients $\boldsymbol{\beta}$ are obtained by solving the regularised least-squares problem

$$\min_{\boldsymbol{\beta}} \sum_{i=1}^{N} (y_i - \boldsymbol{\phi}_i^{\top}\boldsymbol{\beta})^2 + \lambda \parallel \boldsymbol{\beta} \parallel_2^2. \tag{4}$$

The regularisation term controlled by λ mitigates multicollinearity among features and improves model robustness when dealing with noisy industrial data.

To account for potential non-linear relationships between the extracted features and CTWD, SVR is also considered [24]. SVR seeks a function

$$f(\boldsymbol{\phi}) = \mathbf{w}^{\top}\boldsymbol{\phi} + b \tag{5}$$

that deviates from the target values by at most an ε-insensitive margin, while minimising model complexity. This is achieved by solving

$$\min_{\mathbf{w},b,\boldsymbol{\xi},\boldsymbol{\xi}^*} \frac{1}{2} \parallel \mathbf{w} \parallel^2 + C \sum_{i=1}^{N} (\xi_i + \xi_i^*), \tag{6}$$

subject to

$$\begin{aligned} y_i - (\mathbf{w}^{\top}\boldsymbol{\phi}_i + b) &\leq \varepsilon + \xi_i, \\ (\mathbf{w}^{\top}\boldsymbol{\phi}_i + b) - y_i &\leq \varepsilon + \xi_i^*, \\ \xi_i, \xi_i^* &\geq 0. \end{aligned}$$

By introducing kernel functions, SVR implicitly maps the feature vectors into a higher-dimensional space, enabling the modelling of non-linear dependencies between welding signal characteristics and CTWD. In this work, SVR is implemented using a radial basis function (RBF) kernel. The RBF kernel enables the modelling of non-linear relationships between the extracted feature vectors and the CTWD by implicitly mapping the input features into an infinite-dimensional feature space. The kernel function is defined as

$$K(\boldsymbol{\phi}_i, \boldsymbol{\phi}_j) = \exp\left(-\gamma \parallel \boldsymbol{\phi}_i - \boldsymbol{\phi}_j \parallel^2\right), \tag{7}$$

where γ controls the width of the kernel and, consequently, the locality of the regression function. This formulation allows the SVR model to capture smooth and continuous non-linear dependencies commonly observed in welding processes. The regularisation parameter C is used to balance model complexity and training error, while the ε-insensitive loss parameter defines the tolerance margin within

which prediction errors are not penalised. The value of γ is automatically determined by the scikit-learn implementation as a function of the feature dimensionality and data variance.

2.4. 1D-CNN-based CTWD estimation

The proposed feature-based ML paradigm enables the incorporation of signal processing expertise but relies on manual feature design and fixed representations, which may limit its ability to fully capture the complex temporal dynamics present in high-frequency welding signals. Therefore, a DL–based approach is introduced to automatically learn and extract relevant temporal features directly from the welding signal time series, while the ML models serve as baseline methods ranging from simple RLR to more complex SVR.

Neural networks provide an effective mechanism for automatic feature extraction from raw sensory data by learning a non-linear mapping directly from measurements to the target variable [25]. A simple approach for CTWD estimation would be to vectorise a time window of welding signals (e.g., voltage and current) and feed it to a fully-connected neural network (FCNN). However, this strategy presents two major limitations:

- the number of parameters and multiply–accumulate operations increases rapidly with the input dimensionality, leading to an inefficient inference stage; and
- treating each individual time sample as an independent degree of freedom is poorly aligned with the physics of arc welding, where the CTWD is mainly governed by local temporal patterns (e.g., oscillations, transient dynamics, and correlations between voltage/current) rather than by isolated time steps.

For these reasons, we adopt a 1-dimensional convolutional neural network (1D-CNN), which exploits parameter sharing and local receptive fields to extract informative temporal features while maintaining a compact and computationally efficient model [26]. Let us consider a fixed-length temporal window of N samples, such as 1000 of this study. The input to the network is defined as a two-channel tensor

$$\mathbf{x} \in \mathbb{R}^{C\times N}, C = 2, \mathbf{x} = \begin{bmatrix} \boldsymbol{I} \\ \boldsymbol{V} \end{bmatrix}, \tag{8}$$

where $\mathbf{V}, \mathbf{I} \in \mathbb{R}^{N}$ are the sampled sequences. A 1D convolutional layer computes a set of F feature maps $\mathbf{y} \in \mathbb{R}^{F\times N'}$ as

$$y_f[n] = \sum_{c=1}^{C} \sum_{m=0}^{K-1} w_{f,c}[m]\; x_c[n+m-p] + b_f, f = 1, \dots, F, \tag{9}$$

where K is the kernel length, p is the padding size, $w_{f,c}$ are the convolutional weights shared across time, and b_f is the bias term. The resulting representations are passed through a non-linear activation function $\sigma(\cdot)$ (ReLU in this work), yielding

$$\tilde{y}_f[n] = \sigma\big(y_f[n]\big), \tag{10}$$

Thus enabling the extraction of non-linear temporal patterns and cross-channel dependencies between voltage and current. Compared to an FCNN, the 1D-CNN provides a principled inductive bias for time series analysis: kernels act as learnable temporal filters that detect local patterns (e.g., transient

instabilities) while maintaining a bounded computational cost. In this study, we evaluate several candidate configurations and report the best-performing architecture.

2.5. Hyperparameters discovery

As mentioned, selecting the most suitable ML model also requires an appropriate tuning of its hyperparameters. This can be performed either through manual trial-and-error procedures or through automated search strategies, such as grid search. In all cases, the identification of the most appropriate hyperparameter configuration requires a proper separation between training and testing data. The choice of this procedure should depend on the size and composition of the dataset, since the final objective is to identify the model configuration that best generalises to unseen data while ensuring a fair and consistent evaluation framework.

For the feature-based ML models, hyperparameter tuning was carried out through a grid-search procedure implemented in the scikit-learn library. A predefined set of candidate values was specified for each model, and all combinations were systematically evaluated. Model selection was then performed using 5-fold cross-validation (see Figure 4), so that the final hyperparameter configuration was chosen on the basis of the lowest average validation error. In 5-fold cross-validation, the available dataset is divided into five approximately equal subsets. At each iteration, four folds are used for training and the remaining fold is used for validation. This procedure is repeated five times, so that each fold is used once as validation set. The final performance is then computed as the average across the five validation folds.

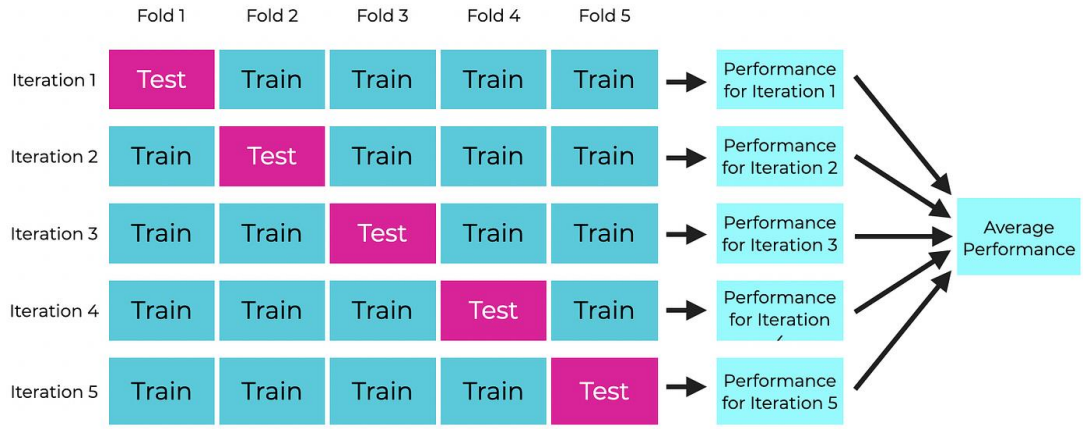

Figure 4. Cross validation procedure employed for testing the model performance across different sub-datasets.

This strategy provides a more robust estimate of generalisation capability than a single train-test split, since it reduces the dependence of the results on a specific partition of the data. This aspect is particularly important for datasets of limited size, such as the one considered in this study, where the number of samples is below 1000. In such cases, the performance estimate can be strongly affected by the specific composition of the training and testing subsets, potentially leading to overly optimistic or overly pessimistic conclusions depending on the particular split. For this reason, cross-validation was adopted as a more reliable strategy for model selection. In the present study, the mean absolute error (MAE) was used as the reference metric for hyperparameter tuning and model comparison.

$$\mathrm{MAE} = \frac{1}{\mathrm{N}}\sum_{i=0}^{N} |\hat{y}_i - y_{target,i}| \quad (11)$$

For Ridge Regression, the regularisation parameter was selected from a logarithmically spaced grid of candidate values. The optimal configuration corresponded to $\lambda = 1$, which was therefore retained in the final model.

For SVR with radial basis function kernel, the grid search explored different values of the regularisation parameter C, the ε-insensitive loss parameter ε, and the kernel parameter γ. The final selected configuration corresponded to $C = 5.0$ and $\varepsilon = 0.01$.

For the 1D-CNN model, hyperparameter selection was carried out through a trial-and-error procedure rather than a full combinatorial grid search, due to the considerably higher computational cost associated with repeated deep-learning training. In particular, the structure of the encoder component, responsible for transforming the high-frequency time series into a lower-dimensional representation, was adopted from a previous study [15,27].

The adopted feature extractor consists of three convolutional blocks with 32, 16, and 8 filters, respectively, kernel size equal to 5, padding equal to 2, and average pooling after each block.

After the convolutional stage, the extracted representation is flattened and passed to a regression head composed of fully connected layers. Different regressor configurations were investigated in this stage in order to assess the effect of model capacity on predictive performance and training stability. In particular, fully connected architectures with hidden-layer sizes [64, 32], [128, 64], and [256, 128] were tested. Among these alternatives, the configuration with two fully connected layers of sizes 256 and 128 provided the most favourable balance between predictive accuracy, convergence stability, and computational cost, and was therefore selected for the final model. The output layer employs a hyperbolic tangent activation function. This choice was motivated by the adopted data normalisation strategy, whereby the input signals were scaled to the range [0,1] and the target CTWD values were scaled to the interval [−1,1]. Under these conditions, the use of a bounded and symmetric output activation was found to be more appropriate for the regression task. In particular, the hyperbolic tangent output yielded more stable optimisation and lower prediction error than the alternative output configurations that were tested. The network was trained using the Adam optimiser with learning rate $\alpha = 0.001$, batch size equal to 32, and 400 epochs. A summary of the hyperparameter search procedure and the final selected configurations for all the considered models is reported in Table 3, while in Figure 5 is shown the final architecture of the proposed 1D-CNN.

Table 3. Feature set adopted for the ML-based CTWD estimation models.

Model	Hyperparameters tested	Final selected configuration
Ridge Regression	$\lambda \in (0.1, 0.2, 1, 2, 10)$ over a logarithmic grid	$(\lambda = 1)$
SVR (RBF)	$(C \in [1, 2, 5, 10])$, $\varepsilon \in [0.05, 0.1, 0.2]$	$(C = 5.0)$, $(\varepsilon = 0.01)$
1D-CNN	Size of fully connected layers, output activation, learning rate, batch size, epochs	3 convolutional blocks (32, 16, 8 filters), kernel size = 5, padding = 2, average pooling, fully connected layers = 256 and 128, tanh output, Adam, learning rate = 0.001, batch size = 32, epochs = 400

Once the best-performing hyperparameter configuration had been identified for each model, the corresponding final model was retrained using the entire available dataset. This choice reflects the intended deployment scenario. Indeed, after model selection has been completed, there is no practical advantage in excluding part of the available data from training, since the objective becomes to maximise the information used to estimate the final model parameters before online implementation. In this sense, cross-validation was employed exclusively for model selection and performance assessment, whereas the final deployed model was trained on all the available samples in order to exploit the full variability of the process and improve robustness during online operation.

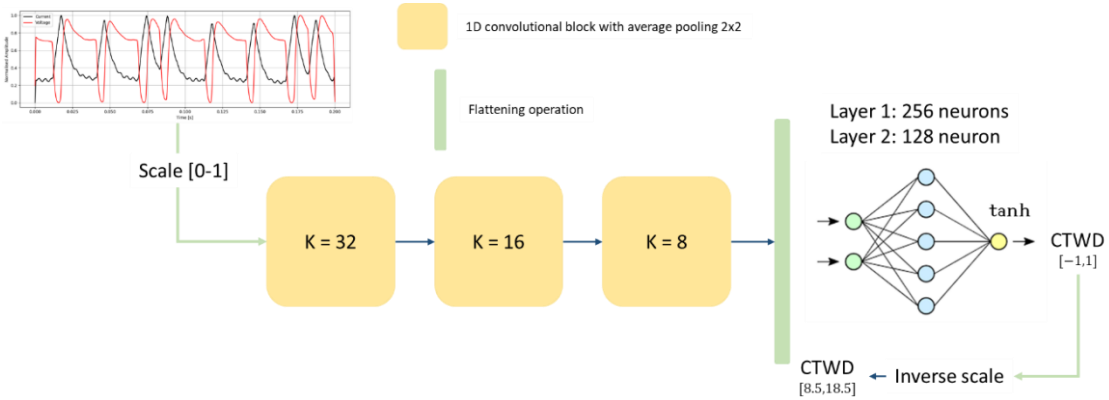

Figure 5. Final architecture of the employed 1D-CNN for the online CTWD estimation.

3. Results

3.1. Comparative analysis of the results

To evaluate the predictive performance of the proposed models while avoiding data leakage and accounting for the limited availability of experimental data, a 5-fold cross-validation procedure was adopted. The dataset was randomly partitioned into five mutually exclusive folds of equal size. At each iteration, four folds (560 samples) were used for model training, while the remaining fold (140 samples) was retained for testing. This process was repeated five times, ensuring that each fold was used once as an independent test set.

Cross-validation was employed to assess the generalisation capability of the models and their ability to estimate CTWD from previously unseen process data. Model accuracy was quantified using the MAE, computed after applying the inverse scaling transformation to the predicted outputs, so that errors were expressed in the original physical units of CTWD.

The MAE values obtained for each fold, together with their mean and standard deviation, are reported in Table 4. A comparative overview of the predictive performance achieved by all the investigated models is provided in Figure 6, highlighting both accuracy and robustness across the cross-validation runs.

Following the assessment of out-of-sample performance, the final model configurations were retrained using the entire available dataset, in order to maximise the amount of information exploited during parameter estimation. The corresponding results, representative of the models employed in the final deployment stage, are reported in Table 4.

Across the validation folds, the SVR achieves the lowest average MAE (0.90 $\pm$0.10 mm), followed by the proposed 1D-CNN (1.13 $\pm$0.05 mm) and Ridge Linear Regression (1.19 $\pm$0.18 mm). However,

the average MAE alone does not fully capture model robustness. In particular, the standard deviation across folds reveals important differences in stability: the proposed 1D-CNN shows the lowest variability, indicating a more consistent performance with respect to changes in the training and test partitions. To further investigate model behaviour, residuals were analysed after retraining each model on the full dataset. Although SVR and Ridge Linear Regression exhibit near-zero mean residuals, both models show substantially larger residual dispersion, with standard deviations of 1.18 mm and 1.85 mm, respectively. This indicates that, despite their low average bias, these approaches remain prone to occasional large estimation errors, sometimes exceeding 1.5 mm.

Table 4. Results of the cross-validation of the proposed indirect CTWD estimator based on deep learning.

Model	Metric	Fold 1	Fold 2	Fold 3	Fold 4	Fold 5	Average	Full-Dataset Residuals (mean + std, mm)
Proposed 1D-CNN	MAE [mm]	1.15	1.15	1.13	1.21	1.04	1.13 ±0.05	0.06 ±0.33
Ridge Linear Regression	MAE [mm]	1.36	1.15	1.06	0.96	1.44	1.19 ±0.18	0.0 ±1.85
Support Vector Regressor	MAE [mm]	1.04	0.97	0.81	0.76	0.89	0.90 ±0.10	0.02 ±1.18

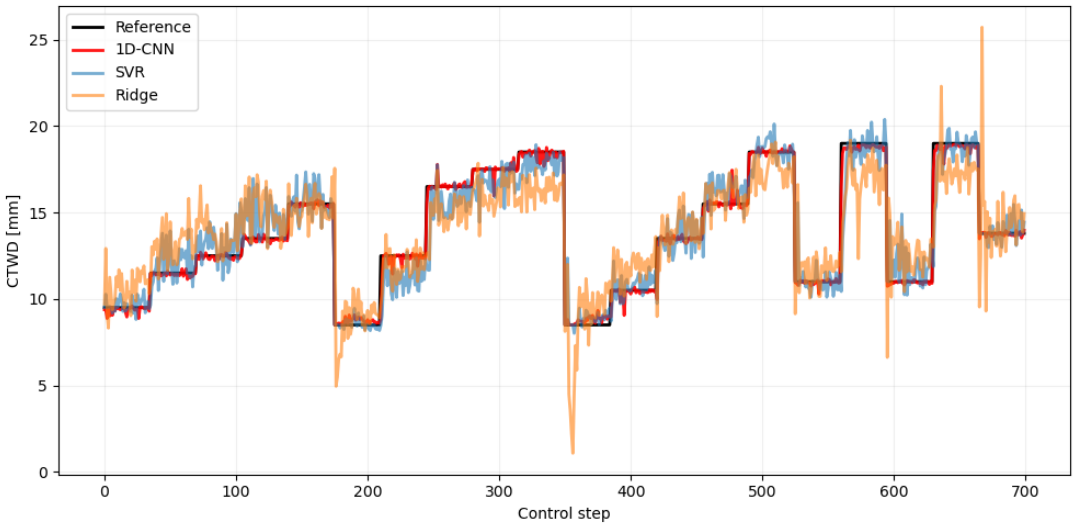

Figure 6. Estimation performance of the proposed ML and DL models.

By contrast, the proposed 1D-CNN yields a residual distribution characterised by both a low mean error (0.06 mm) and a markedly smaller standard deviation (± 0.33 mm). Although its mean bias is slightly higher than that of SVR (0.02 mm), this difference is negligible from a practical perspective. More importantly, the much lower residual variance suggests that the proposed model provides more reliable and bounded estimations. For process monitoring applications, such behaviour is preferable to models that may achieve lower average error but are also more susceptible to sporadic large deviations. Consequently, the proposed 1D-CAE is selected as the most suitable estimator for indirect CTWD monitoring, as it provides a more reliable and robust behaviour under realistic process variability.

3.2. Example of process stability monitoring application with the proposed methodology

Once the CTWD is estimated online from voltage and current signals using the proposed model, the resulting sequence of estimates can be directly exploited for statistical process monitoring (SPM). In this

work, an Exponentially Weighted Moving Average (EWMA) control chart is adopted as an illustrative example of how the estimated CTWD can be used to supervise process stability during wire-based deposition. The EWMA statistic is defined as

$$Z_t = \alpha \widehat{\mathrm{CTWD}}_t + (1-\alpha) Z_{t-1}, \tag{12}$$

where $\widehat{\mathrm{CTWD}}_t$ is the estimated CTWD at time t, $\alpha \in (0,1]$ is the smoothing factor, and Z_0 is initialised to the nominal CTWD value. In this study, $\alpha = 0.2$ was selected as a compromise between sensitivity to slow drifts and robustness to measurement noise, which is particularly relevant in welding processes where local waveform distortions and arc instabilities can induce short-term fluctuations in the estimated signals. Control limits were defined based on process stability considerations rather than purely statistical thresholds. Specifically, an acceptable operating bounds were set to ± 2.8 mm, yielding lower and upper limits of 11.8 mm and 15.8 mm, respectively. These limits reflect practical constraints on heat input and arc stability, ensuring that excessive variations in CTWD do not compromise deposition quality.

Figure 7 illustrates the application of the proposed EWMA-based monitoring strategy during an open-loop deposition experiment. The light-blue signal represents the instantaneous CTWD estimates obtained from the 1D-CNN, while the red curve shows the corresponding EWMA-filtered trend. The nominal CTWD value and stability bounds are also reported. The experiment consisted of printing a single-wall structure (see Figure 7b). During deposition, the value of layer height was kept constant at 2.2 mm (from previous works this is the expected value for this set of parameters) and no feedback control was applied to the torch height, resulting in uncontrolled variations of the actual CTWD. As shown in Figure 7a, the CTWD exhibits significant variability during the process and a progressive upward drift towards the final stages of the build.

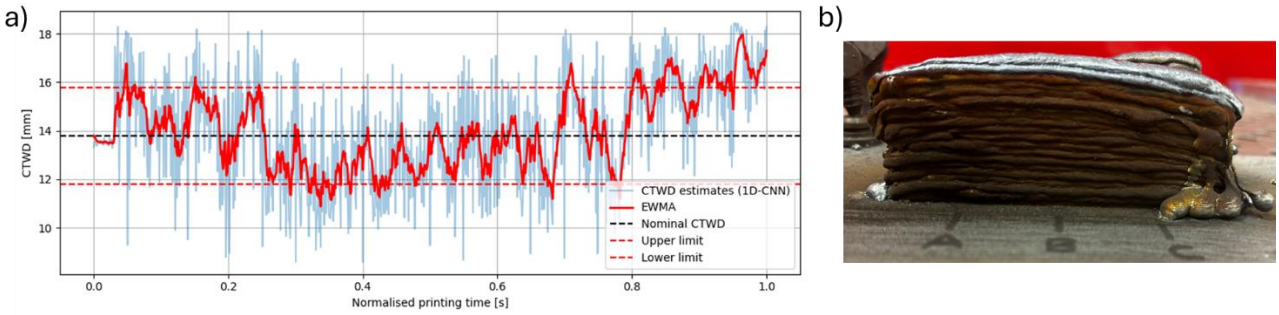

Figure 7. Example of EWMA-based process monitoring enabled by the proposed CTWD estimator. **(a)** Time evolution of the estimated CTWD during an open-loop deposition experiment; **(b)** Single-wall structure produced during the experiment, showing geometric instabilities and uneven layer formation associated with uncontrolled CTWD variations.

These effects are primarily attributed to the accumulation of geometric errors: layer height fluctuates around the nominal value, sometimes exceeding 2.2 mm and sometimes remaining below it, while the torch position is not adjusted accordingly. Over multiple layers, this mismatch leads to increasing deviations in CTWD, which in turn affect heat input, melt pool stability, and final part geometry, resulting in uneven layer formation and structural defects, as visible in the deposited wall.

The EWMA control chart clearly highlights these trends by filtering out high-frequency noise and emphasising slow drifts, enabling early detection of process degradation.

This example demonstrates how the proposed CTWD estimator, combined with a simple SPM tool, can support real-time quality monitoring and provide a foundation for future feedback control strategies aimed at stabilising arc geometry and improving process repeatability.

3.3. Additional discussion and future research direction

The results presented in this study should be interpreted as a first step towards a broader signal-driven framework for process understanding and supervision in WA-DED. The main contribution of the work is not limited to the estimation of CTWD itself, but also lies in the systematic comparison of modelling strategies with increasing levels of representational complexity. In particular, the study compares classical ML approaches based on manually extracted features with a deep learning approach capable of learning directly from raw high-frequency welding signals. Beyond predictive performance alone, this comparison provides useful insight into whether linear, non-linear, or more expressive data-driven models are better suited to describing the relationship between welding dynamics and CTWD.
From this perspective, the findings suggest that:

- Raw-data modelling is a promising direction for intelligent manufacturing applications, as it may reduce the need for manual feature engineering while still capturing relevant process information. This aspect is particularly important in industrial environments, where robust and scalable data pipelines are often preferred over approaches requiring extensive signal pre-processing and expert-driven feature definition. The present work therefore contributes to the development of a methodology in which CTWD can be inferred directly from electrical process signals, opening the way to more automated and adaptive monitoring strategies.
- CTWD estimation can be used within a qualification-oriented process monitoring framework. In WA-DED, once a suitable set of process parameters has been identified to achieve a desired thermal condition or deposition regime, it becomes important to maintain those conditions as consistently as possible throughout the build. Since CTWD is strongly connected to arc behaviour and heat transfer conditions, its reliable estimation may provide an indirect but meaningful indicator of process drift. The proposed method could support the identification of out-of-specification operating conditions.
- Such information could be used to alert the operator, interrupt the deposition, and recalibrate the stand-off condition before proceeding with the subsequent layer. In this sense, the methodology may be valuable even in the absence of full closed-loop control, as it can still provide an actionable diagnostic tool for preventing the accumulation of geometric or thermal deviations during multi-layer deposition.

At the same time, the present study does not propose a feedback controller, and this limitation should be explicitly acknowledged. Although one possible future direction would be to use CTWD estimation as the basis for automatic control, a direct implementation of a conventional PID strategy driven by instantaneous regression error may not be the most appropriate solution. The reason is that the estimated CTWD remains affected by several sources of variability, including signal noise, process stochasticity, and the inherent fluctuations of metal transfer dynamics, especially in standard gas metal arc welding regimes such as short-circuit transfer. Under these conditions, the relationship between the measured electrical signals and the true CTWD is not fully deterministic, and similar CTWD values may

correspond to partially different signal realisations. As a consequence, control actions based on instantaneous estimates alone may be overly sensitive and may lead to unstable or suboptimal corrections.

For this reason, alternative supervisory and control strategies deserve further investigation:

- A first option would be to smooth or average the estimated CTWD over an appropriate temporal window and apply corrections at discrete intervals, for example on a layer-by-layer basis, rather than continuously during deposition. Such a strategy may be more compatible with the dynamics of WA-DED and less sensitive to short-term process fluctuations and therefore noisy estimates.
- A second possibility would be to reformulate the task from continuous regression to discrete classification, for instance by identifying whether the process is within the acceptable CTWD range, approaching a warning threshold, or outside specification. This type of formulation may be particularly attractive in industrial settings, where decision-making often relies more naturally on operational states than on precise point estimates. A further extension could involve stochastic or probabilistic modelling approaches capable of explicitly accounting for uncertainty in the input-output relationship, thereby representing not only an estimated CTWD value but also the confidence associated with that estimate.

Finally, the generalisability of the proposed models remains an open research question and should be explored more thoroughly in future work. The present analysis is based on a specific experimental setting, and broader validation is needed to assess how well the different modelling approaches transfer across changes in process parameters, alloys, welding transfer modes, torch configurations, and deposition strategies. Extending the analysis in this direction would strengthen the practical relevance of the framework and help define the limits within which raw-signal CTWD estimation can be robustly applied.

4. Conclusion

This work demonstrates that the CTWD during a WA-DED process can be reliably estimated from standard welding sensor signals, namely voltage and current, using data-driven approaches. The proposed method, based on a 1D-CNN architecture, enables indirect CTWD estimation without additional sensing hardware, providing a practical solution for industrial welding and additive manufacturing environments.

The experimental results show that the proposed estimator achieves a mean error of 0.06 mm with a standard deviation of 0.48 mm over a CTWD operating range of approximately 10 mm. Cross-validation analysis further confirms the robustness of the approach, with a stable mean absolute error across folds and a markedly lower residual variance compared to linear and kernel-based regression models. Although alternative methods, such as Machine Learning-based Linear Ridge Regression and Support Vector Regression, exhibit marginally lower bias on average, their significantly higher error dispersion leads to occasional deviations exceeding 1.5 mm, which are undesirable in process monitoring applications. In contrast, the proposed model ensures a consistent estimation accuracy within an acceptable error band, a property that is critical for reliable industrial deployment.

From an application perspective, the availability of an online CTWD estimate enables process monitoring and supervision, for instance, through the integration of the estimated CTWD into control charts to track deposition quality during manufacturing. Moreover, the achieved accuracy is sufficient to support feedback control strategies, where the estimated CTWD can be used to adjust torch positioning in real time. These capabilities open the way to closed-loop control architectures aimed at improving process stability and repeatability.

The main limitation of the present study lies in the validation being conducted on a single process parameter set, which restricts the immediate generalisation of the results. However, this limitation does not undermine the applicability of the proposed framework. Extending the method to different parameter configurations primarily requires repeating the calibration procedure and reoptimising the network hyperparameters, without altering the underlying architecture. As such, the approach remains inherently scalable and suitable for industrial adoption. Future work will focus on validating the method across multiple process conditions and materials, as well as on the integration of the proposed estimator into a fully closed-loop control system for CTWD regulation in robotic welding and wire-based additive manufacturing processes.

Data availability statement

The data or datasets that support the findings of this study are available from the corresponding author upon reasonable request.

Declaration of generative AI and AI-assisted technologies

During the preparation of this manuscript, the authors used generative AI tools (ChatGPT) only to grammar refinement, improve language and readability. The authors take full responsibility for the content of the manuscript.

Acknowledgments

The authors acknowledge the financial support of the INVITALIA project NEMESI (CUP C67G22000420008) in the development of this research.

Authors' contribution

Conceptualization, G.M. and E.M.; methodology, G.M. and E.M.; software, G.M. and E.M.; validation, G.M. and E.M.; formal analysis, G.M., E.M., L.N. and J.X.; investigation, G.M., E.M., L.N. and J.X; resources, G.M. and L.N.; data curation, G.M., E.M.; writing—original draft preparation, G.M., E.M., L.N. and J.X; writing—review and editing, G.M., E.M., L.N. and J.X; visualization, G.M., E.M., L.N. and J.X; supervision, L.N. and J.X; project administration, G.M., and J.X; funding acquisition, L.N. All authors have read and agreed to the published version of the manuscript.

Conflicts of interest

Giulio Mattera and Jinyang Xu holds the position of Editorial Board Members for *AI & Materials* and has not peer reviewed or made any editorial decisions for this paper.

References

[1] Pan Z, Ding D, Wu B, Cuiuri D, Li H, *et al*. Arc welding processes for additive manufacturing: a review. *Trans. Intell. Weld. Manuf.* 2018, 1:3–24.

[2] Lambiase F, Yanala P, Pace F, Andreucci E, Paoletti A. A state of the art review of wire arc additive manufacturing (WAAM)–part 1: process fundamentals, parameters and materials. *Int. J. Adv. Manuf. Technol.* 2025, 138:11, 4965−4993.
[3] Gao H, Li H, Shao D, Fang N, Miao Y, *et al*. Towards quality controllable strategies in wire-arc directed energy deposition. *Int. J. Extrem. Manuf.* 2025, 7(4):042004.
[4] Li B, Zhang X, Li W. Exploratory study of repairing damaged aluminum part through robotic hybrid wire arc additive manufacturing and machining for potential in-space manufacturing. *Int. J. Adv. Manuf. Technol*. 2024, 135:3101–3112.
[5] Mattera G, Manoli E, Nele L. Study on the printing stability of Invar 36 alloy under different process parameter conditions in gas metal arc additive manufacturing. *Mater. Sci. Addit. Manuf.* 2025, 4:025220046.
[6] Teng S, Dehgahi S, Henein H, Wolfe T, Qureshi A. Sensor-fusion enabled inter-layer temperature control of nano-treated 7075 aluminum alloy produced through wire-arc directed energy deposition process. *Prog. Addit. Manuf.* 2025, 10(2):1293–1314.
[7] Cui J, Yuan L, Commins P, Cui J, He F, *et al*. WAAM process for metal block structure parts based on mixed heat input. *Int. J. Adv. Manuf. Technol.* 2021, 113:503–521.
[8] Mattera G, Manoli E, Pan Z, Nele L. Process monitoring of P-GMAW-based wire arc direct energy deposition of stainless steels via time-frequency domain analysis and Isolation Forest. *Adv. Manuf*. 2025, 2(2):0010.
[9] Hölscher L, Hassel T, Maier H. Detection of the contact tube to working distance in wire and arc additive manufacturing. *Int. J. Adv. Manuf. Technol.* 2022, 120:989–999.
[10] Chabot A, Rauch M, Hascoët J. Novel control model of Contact-Tip-to-Work Distance (CTWD) for sound monitoring of arc-based DED processes based on spectral analysis. *Int. J. Adv. Manuf. Technol.* 2021, 116:3463–3472.
[11] Shi M, Xiong J. Controlling torch height and deposition height in robotic wire and arc additive manufacturing on uneven substrate. *Weld. World* 2024, 68:765–779.
[12] Zhu X, Yu J, Liu Y, Song Y, Zhang L, *et al*. Application of artificial intelligence combined with density functional theory in materials. *AI Mater*. 2026, 2(1):0001.
[13] Quagliato L, Seitz J, Perin M. Machine learning modeling for material science and manufacturing: overview and perspectives for the future. *AI Mater*. 2025, 1(1):0005.
[14] Mattera G, Chozaki S, Norrish J. Advances in machine learning for parameters optimisation and *in-situ* monitoring of wire arc additive manufacturing. *Weld. World* 2025, 1–30.
[15] Mattera G, Vozza M, Polden J, Nele L, Pan Z. Frequency informed convolutional autoencoder for *in situ* anomaly detection in wire arc additive manufacturing. *J. Intell Manuf.* 2024, 36(8):5819–5834.
[16] Khanna N, Gandhi A, Nakum B, Srivastava A. Optimization and analysis of surface roughness for INVAR-36 in end milling operations. *Mater. Today Proc.* 2018, 5:5281–5288.
[17] Huang G, He G, Gong X, He Y, Liu Y. Additive manufacturing of Invar 36 alloy. *J. Mater. Res. Technol.* 2024, 30:1241–1268.
[18] Veiga F, Suárez A, Artaza T, Aldalur E. Effect of the heat input on wire-arc additive manufacturing of Invar 36 alloy: microstructure and mechanical properties. *Weld. World* 2022, 66:1081–1091.

[19] Iturrioz A, Ukar E, Pereira J. Influence of the manufacturing strategy on the microstructure and mechanical properties of Invar 36 alloy parts manufactured by CMT-WAAM. *Int. J. Adv. Manuf. Technol.* 2025, 136:729–744.

[20] Ye S, Xu L, Guo Y, Di X, Han Q, *et al.* Microstructure and mechanical properties of super-invar alloy fabricated by wire-arc additive manufacturing. *Adv. Manuf.* 2025, 2(1):0005.

[21] Alcaraz J, Foqué W, Sharma A, Tjahjowidodo T. Indirect porosity detection and root-cause identification in WAAM. *J. Intell. Manuf.* 2024, 35(4):1607–1628.

[22] Alcaraz J, Sharma A, Tjahjowidodo T. Predicting porosity in wire arc additive manufacturing (WAAM) using wavelet scattering networks and sparse principal component analysis. *Weld. World* 2024, 68:843–853.

[23] Surovi N, Soh G. Acoustic feature based geometric defect identification in wire arc additive manufacturing. *Virtual Phys. Prototyp.* 2023, 18(1):e2210553.

[24] Ding D, He F, Yuan L, Pan Z, Wang L, *et al.* The first step towards intelligent wire arc additive manufacturing: An automatic bead modelling system using machine learning through industrial information integration. *J. Ind. Inf. Integr.* 2021, 23:100218.

[25] Xiong P, Wang H, Liu M, Liu X. Denoising autoencoder for eletrocardiogram signal enhancement. *J. Med. Imaging Health Inform.* 2015, 5(8):1804–1810.

[26] Kuester J, Gross W, Middelmann W. 1D-convolutional autoencoder based hyperspectral data compression. In *Proceeding of the XXIV ISPRS Congress*, Online, July 5–9, 2021, pp. 15–21.

[27] Mattera G, Mattera R, Otto P. Hybrid statistical process monitoring of wire arc additive manufacturing with frequency-informed deep learning. *Qual Reliab Eng. Int.* 2025, 41(8):3334–3349.